Applied and Computational Mechanics 17 (2023) 93–104

Design and optimization of squirrel cage geometries in aircraft engines toward robust whole engine dynamics

I. Chatzisavvas[a,*], I. Arsenyev[a], R. Grahnert[a]

[a]*MTU Aero Engines AG, Dachauer Straße 665, 80995 Munich, Germany*

Received 27 May 2023; accepted 28 November 2023

Abstract

In this work, an coupled end-to-end approach for the optimization of the rotor dynamic behavior of a dual-spool aircraft engine along with fatigue life optimization of squirrel cages (SQC) is presented. A realistic model to simulate the rotor dynamics is created, where the high-pressure (HP) rotor is supported by two squirrel cages. The aim of this work is to find a robust rotor dynamics design by shifting a critical speed to higher rotational speed, and at the same time improving the squirrel cage design with respect to fatigue life.

Fully automatized coupled analysis process chain is implemented, allowing to compute the influence of the SQCs geometry variation onto the full rotor dynamics and structural performance of the SQC. Two global optimization techniques are employed to explore the SQCs design space and find optimal 3D geometries, using the aforementioned coupled process.

Optimization results are compared and discussed in detail, indicating the importance of the numerical optimization to improve fatigue life of the squirrel cage. It is shown that optimized and non-optimized SQC designs, both fulfilling rotor dynamics goals, can have significantly different performance regarding their fatigue life. Moreover, the advantage of the coupled process is illustrated, allowing to find superior SQC designs by considering both disciplines simultaneously in comparison with a sequential (uncoupled) approach, when the target elastic properties of an SQC, selected only based on the rotor dynamics requirements, may lead to sub-optimal fatigue life.

Keywords: jet engines, rotor dynamics, squirrel cage, optimization, vibration

1. Introduction

Aircraft engines for civil and military applications are designed to avoid excessive vibrations, which may limit their mechanical integrity as well as their performance. In the concept phase, it is a common practice to shift some critical speeds of the engine, which occur usually due to rigid or flexural (bending) vibration modes of the rotors, into speed ranges that might have a lighter impact on the engine vibrations. In order to achieve this, the stiffness of the rotor supporting elements can be adjusted by modifying the squirrel cage (SQC) centering springs. SQCs are widely used for aircraft engines for improved rotor dynamics and provide the possibility of shifting rigid body as well as flexural modes.

A common approach consists in separating system-level rotor dynamics design to find appropriate elastic properties of rotor supports from the design of particular elements, such as SQCs, to meet these properties and additional (usually fatigue life) goals. Multiple research works focus on either level: rotor system dynamics design by varying integral parameters (stiffness, clearance, etc.) of the dampers (see, e.g., [4]) or finding optimal SQC shape to meet required stiffness and fulfill fatigue goals. For example, [13] iteratively improved an aero-engine

*Corresponding author. Tel.: +49 148 994 04, e-mail: ioannis.chatzisavvas@mtu.de.
https://doi.org/10.24132/acm.2023.841

SQC design to meet the strength, stiffness and fatigue life requirements by modifying baseline design manually based on 3D simulation results. The authors of [15] coupled 3D finite-element structural analysis with a genetic algorithm to find optimal slots shape to reduce stresses and meet the stiffness requirements of an SQC.

The drawback of the outlined two-stage design approach lies in the fact that multiple combinations of SQCs stiffness values exist (especially when multiple SQCs are present on the system), which satisfy the rotor dynamics, but at the same time have different possible fatigue life. Experience-based selection of the stiffnesses may lead to sub-optimal structural performance of the SQCs. This issue is addressed by [16], where the effect of changing the SQC shape parameters is propagated into the dynamic analysis of the rotor, thus, allowing simultaneous SQC design evaluation with respect to system dynamics and fatigue. This coupled approach is paired with multi-objective optimization to find optimal SQC design for an academic-size rotor model. However, the use of approximate analytic equations for stiffness and stress, suitable only for the basic SQC geometry parameterization defined in the paper, makes an application to the industrial-size problem difficult.

In this work, a detailed end-to-end approach for robust engine dynamics is presented and applied to a realistic dual-spool aircraft engine. Multiple geometry parameters are used to describe the SQC shape. To simulate the effect of the SQCs design changes, a simplified modeling of full rotor dynamics is coupled with detailed 3D structural FEM simulations for each of the two SQCs. Global numerical optimization is employed to explore the design space and find optimal 3D SQCs geometries, which satisfy rotor dynamics goals and improve structural life.

The following work is structured as follows: In Section 2, the rotor dynamics model of a realistic aircraft engine is presented. This model will be used for the optimization procedure. In Section 3, the parametric FEM modeling is presented. This fully-parametrized SQC model enables the efficient optimization approach. In Section 4, the coupled optimization procedure is presented. In Section 5, the squirrel cages are optimized and the results are presented. In Section 6, the fatigue of four squirrel cage designs are presented, illustrating the advantages of the coupled optimization approach. Finally, in Section 7, the conclusions of this work are presented.

2. Rotor dynamics model of a realistic aircraft engine

A rotor dynamics model of a realistic aircraft engine is shown in Fig. 1. The system consists of two rotors, the low-pressure (LP) and the high-pressure (HP) rotor. A simplified casing is attached to the model. The rotors are rotating in the opposite direction, assuming that the LP is rotating about the positive z-axis and the HP about the negative z-axis. It is also assumed that their speed ratio is constant over the whole speed range of the engine, an assumption that is not limiting the generality of the proposed optimization approach. The HP rotor is supported by two squirrel cages SQC1 and SQC2, as illustrated in Fig. 1. The stiffness of both SQCs can be varied independently to modify the critical speed of the rotor.

The rotors and the casing are modeled using Timoshenko beam elements with 4 degrees of freedom (DoFs) at each node. The axial and torsional DoFs are neglected in this study. Torsional DoFs are usually uncoupled from the lateral DoFs, and therefore, play no role in this study. A coupling between the axial and the lateral DoFs is usually present due to gas loads, mainly through the main bearings of the engines. In the rotor dynamics context, they can be considered as external loads and the current study can be easily extended to include this scenario. Although it is well known that the linear Timoshenko beam elements are not

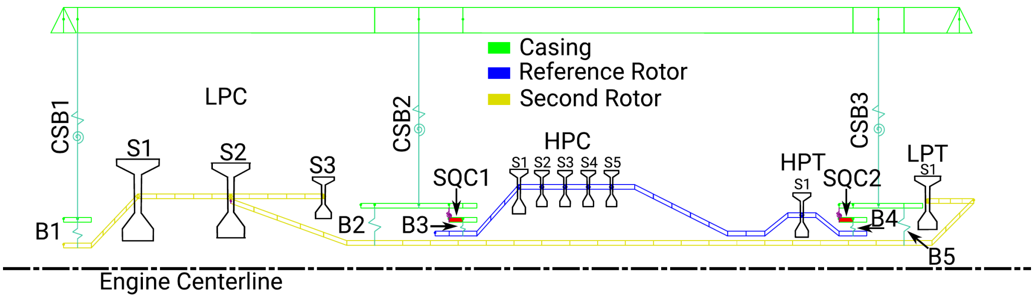

Fig. 1. Rotor dynamics model of a realistic aircraft engine

capable of modeling conical cross sections [2, 6], they are used here for simplicity to avoid 3D or reduced 3D structures.

3. Squirrel cage parametric modeling

Squirrel cages are used for supporting rotors to provide them a soft support that can shift unwanted rigid or flexible modes that lie in the operating range. In this work, a parametrized 3D model of the squirrel cage is used, as shown in Fig. 2. Differently from the work [15], no complex free-form geometries can be represented by this model, however, this parameterization closely represents standard manufacturable SQC design. The model allows changing the number of bars, sizing of bars and modifying the shape of the elliptical fillets. As also noted by [15], the transition region of a small circular arc on the bars often leads to a stress concentration and increased risk of fatigue cracks. Thus, a more flexible elliptical (compared to circular) parameterization is used for fillets here. The geometric parameters and their allowed ranges are listed in Table 1. Given the parameter values, a full 3D SQC model is automatically generated together with a structured hexahedral mesh. A completely new mesh is created at each optimization step, as the method is not based on any kind of mesh morphing technique.

The SQC is assumed to be manufactured from steel having elastic material properties with the Young's modulus E of 210 GPa and Poisson ratio ν of 0.3. As the weight of the squirrel cage is not included in the optimization, the material density of the squirrel cage is not required.

4. Squirrel cage coupled analysis

To enable SQC geometry optimization, a fully automatized multi-disciplinary process chain is implemented, which includes geometry generation and 3D FEM simulation of each SQC as well as rotor dynamics simulation (in this case the critical speed analysis) of the full system. The stiffness of each SQC is obtained from the FE analysis and propagated into the critical

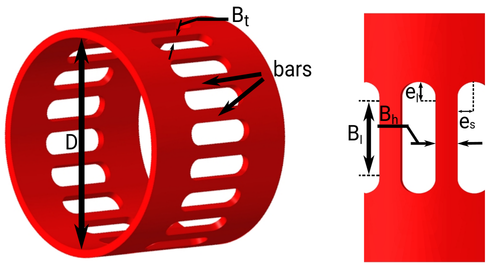

Fig. 2. Squirrel cage dimensions for the parametric modeling and optimization

Table 1. Squirrel cage parameters used for the optimization

Parameter	Description	Unit	min	max
N_{bars}	number of bars	–	20	30
D	outer diameter	mm	160	210
B_t	bar thickness	mm	4	7
B_h	bar height	mm	6	12
B_l	bar length	mm	40	60
e_s	short ellipse	mm	3	8
e_l	long ellipse	mm	8	12

speed simulation, enabling a direct assessment of the influence of the SQC geometry on the system dynamic behavior. FEM simulations, being the most computationally demanding part of the process, are performed in parallel for all SQCs. Currently, the process chain (Fig. 3) provides only zero-order information for output values, so the gradients are not available.

4.1. Critical speed analysis

Critical speed analysis is a special form of eigenfrequency analysis, where the rotational speed equals the orbiting frequency of the mode [5]. The analysis performed here is undamped since the damping will have only a small impact on the critical speeds. The stiffness values of all bearings are considered to be speed-independent. For this rotor, there exist several critical speeds. In this case, only one mode is selected for the optimization, but this assumption is not necessary for the optimization procedure. The rotor mode to be optimized is shown in Fig. 4, together with its undeformed configuration. For clarity, only the deformation of the HP rotor is shown in Fig. 4. Regarding this mode, the LP rotor has almost no deformation. This mode can be characterized as an almost rigid body mode having a conical shape (gyroscopic conical mode). Depending on the SQC stiffness values, the critical speed as well as the shape of this mode can be significantly changed. After the analysis, it can be observed that at the SQC positions, there is an important amount of displacement. Therefore, it is clear that by changing the SQC stiffness values, the mode is expected to be influenced. Another indicator of the importance of the SQCs in this mode is their high strain energy percentage.

It should be noted that the squeeze film damper is neglected in the current analysis. It is known that it produces nonlinear (dynamic) stiffness and damping, so it is included in op-

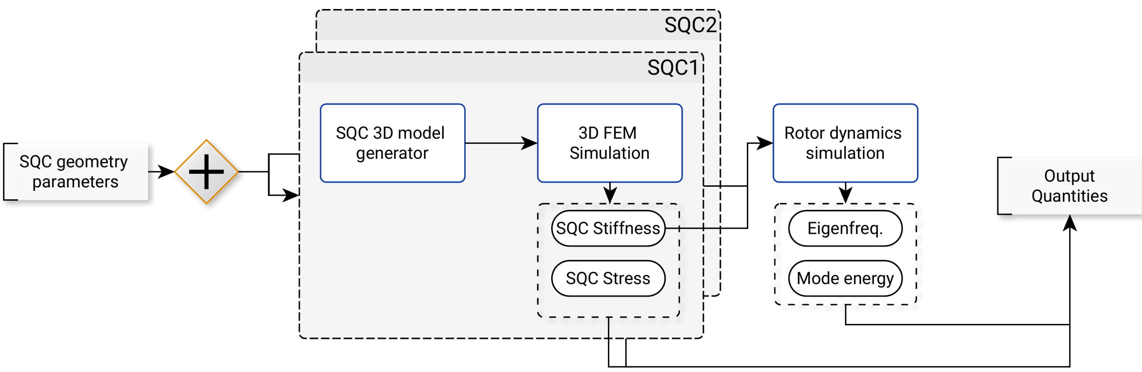

Fig. 3. Coupled analysis process chain

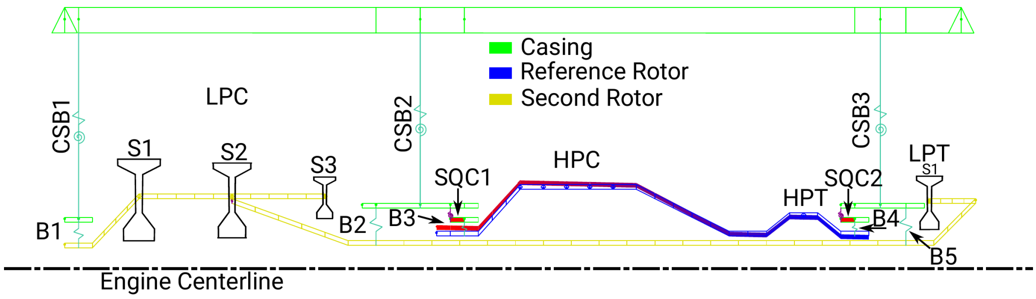

Fig. 4. HP rotor mode together with its undeformed configuration

timization procedures in the more detailed design phases, where nonlinear analyses such as harmonic balance or nonlinear time-transient analysis are used.

Fig. 5 shows the Campbell diagram before the optimization of the SQCs, using 80 kN/mm as stiffness values for both SQCs.

4.2. *Squirrel cage stiffness and stress calculations*

A linear elastic static calculation is performed for every squirrel cage using FEM. The calculations are performed with the CalculiX [3] software, using linear hexahedral finite elements. The squirrel cage is fixed on one side (flange) and a force is applied at the position of the rolling element bearing. The fixation points and the force application points are indicated in Fig. 6. In this way, its stiffness is calculated. It should be noted that the radial stiffness of the SQC may vary depending on the direction of the applied force. If the radial force is applied towards the middle of a bar, the stiffness will be higher than if the force is applied in the direction between two bars. However, due to the large number of bars, this stiffness variation is insignificant in our case and is therefore neglected.

In the following work, the SQC is assumed to be isotropic. The simulation time for one calculation is less than 2 minutes with a standard computer. At the same time the stresses are also evaluated and scaled according to the maximum allowed radial displacement of the squirrel cage, which corresponds to the squeeze film damper gap. For the stress values, the worst principle stresses are used as the structural design goal, however, the same procedure can be used with the von Mises equivalent stress or any other formulation. The deformed squirrel cage and the distribution of the worst principle stress are shown in Fig. 6. From the presented distribution, it is clear that the stresses are concentrated in the elliptical fillet regions. The deformation of the squirrel cage takes place mainly at the flexible bars, as expected. The area left and right of the bars undergoes almost zero rotation and deformation.

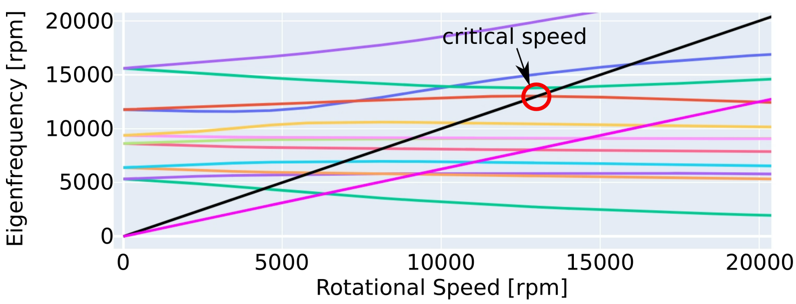

Fig. 5. Campbell diagram of the rotor/bearing/casing system before the optimization

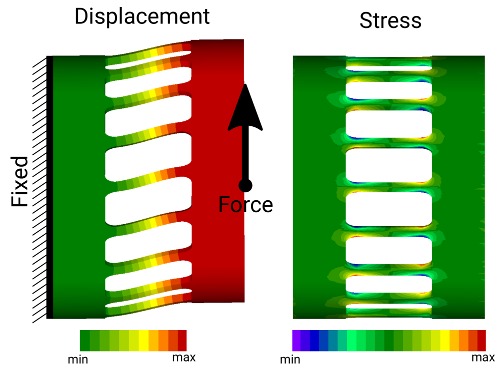

Fig. 6. Displacement and stress of a squirrel cage under static load

5. Squirrel cage optimization

In order to find the best possible SQCs design, the developed multi-disciplinary process chain, considered here as a black-box, is coupled with a numerical optimization method. The goal of the optimization is to find 3D SQCs geometries (which follow the described above parametrization) which fulfill rotor dynamics constraint(s) and yield the lowest structural stresses to improve fatigue life. Regarding rotor dynamics, a conical mode, which lies in the speed range of the HP rotor idle speed, should be shifted towards higher rotational speeds. The definition of the optimization problem objective and constraints is summarized in Table 2. The strain energy of the conical mode is given as a percentage of the total strain energy of the system, which adds up to 100 %. The parameters of each of the two squirrel cages can be changed independently, so in total there are 14 design variables available. Two problem formulations are considered within this work, with a constant (nominal) number of bars ($N_{bars} = 22$), which reduces the number of variables to only 12 and with a variable number of bars. Due to the absence of gradient information and relatively low problem dimension, direct (zero order) optimization methods are used to solve the problem. Moreover, the number of bars, being an integer parameter, requires some special treatment within optimization.

Adaptive surrogate-based global optimization tool AutoOpti [1, 12], which is based on the efficient global optimization [10] concept is used in this study. This optimization strategy consists of initial sampling, (re)fit of the surrogate models for each response, searching for the next promising point(s) based on infill criteria, evaluating these points using true simulations and augmenting the set of training points with the obtained results. All these steps, except the initial sampling, are repeated until the convergence criterion is fulfilled. Latin-Hypercube Sampling (LHS) [8] is used to generate designs for fitting the initial Kriging models, which has better space-filling properties than a random sampling. The key ingredient here is the infill criterion – the Expected Improvement (EI) [10], which provides the balance between exploration and ex-

Table 2. Squirrel cage optimization problem

Quantity	Type	Units	Goal
maximum stress in the SQCs	objective	MPa	minimize
critical speed (conical mode)	constraint	rpm	higher than 12 000
strain energy of the conical mode	constraint	%	less than 5
SQC stiffness	constraint	kN/mm	within $[20, 80]$

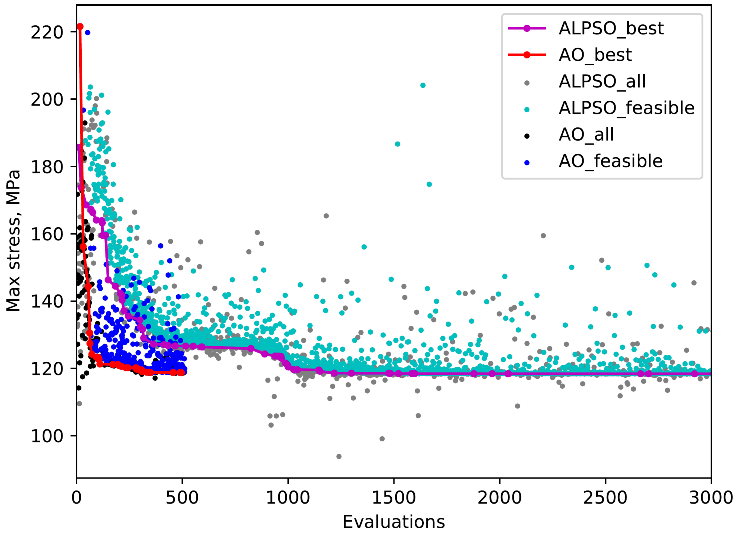

Fig. 7. Reduction of maximum stress in SQCs by AutoOpti and ALPSO optimizers with $N_{bars} = 22$

ploitation properties. For more details, for example, about constraints handling or infill search, the readers are referred to [1, 12]. For the sake of comparison, another zero-order optimization method, the Particle Swarm Optimization, is considered in this work. A combination of Particle Swarm Optimization with Augmented Lagrangian Penalty function (ALPSO) to handle general non-linear constraints, proposed in [7], is used in this work, with an implementation based on pyOpt [9]. Thus, the method combines capabilities of the particle swarm method to find global optimum in complex problems with accurate constraints handled by using the Augmented Lagrange multiplier method [7].

Optimization results for the constant number of bars are shown in Fig. 7, where the history of the objective function, the maximum worst principal stress over both SQCs, is plotted over the number of evaluated designs. For each of the methods, three sets of design points are plotted: solutions improving the design with respect to the best known ("best"), points which fulfill all the constraints ("feasible") and other designs explored by the method. The frequency constraint is active at the optimum with the critical frequency equal to 12 000 rpm. Considering optimization performance, both methods converged to essentially the same solution, however, AutoOpti needed much fewer design evaluations and approx. 2 hours of a wall time for the whole optimization. Actually, optimization could have been stopped earlier, as almost optimal solutions were found already by AutoOpti within the first 100 evaluations (approx. 30 min) with a rather slow improvement afterwards.

Independently from the optimizer, both SQCs have nearly the same optimal stiffness (see Fig. 8) and design, indicating that such a solution (with equal stiffness) is acceptable for the rotor dynamics. Thus, the optimal SQCs tend to have the same maximum stresses, which follows from the fact that both squeeze film dampers have the same clearance. This would allow using the same SQCs at both locations, reducing manufacturing and maintenance costs.

Thanks to the fact that both methods, AutoOpti and ALPSO, support non-categorical integer design variables, the number of bars N_{bars} can be also used as an optimization variable. Results of both methods are shown in Fig. 9. As for the constant number of bars, "all", "feasible", and "best" points are plotted. Results of the methods indicate that a higher number of bars is preferable for the current problem setting and the number of bars is increased to 30, which is the design upper bound. Compared to the best design with $N_{bars} = 22$, increasing the number

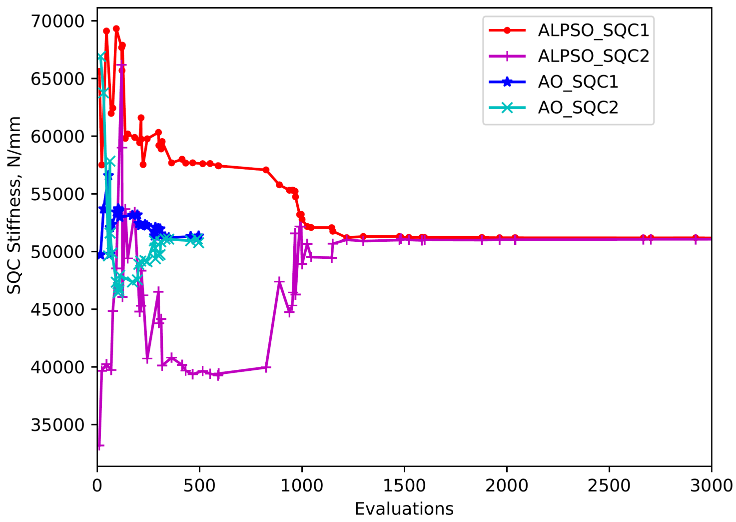

Fig. 8. Stiffness evolution of both SQCs during optimization with $N_{bars} = 22$

of bars to 30 further reduces the maximum stress by approx. 17 MPa, or 14 %.

To illustrate the advantage of the coupled optimization, another combination of SQCs stiffnesses (75 and 14 kN/mm, respectively) was selected, which satisfies the rotor dynamics goals, is taken for optimization. This corresponds to an approach when stiffnesses are selected first based on rotor dynamics only, and each SQC is then optimized to meet the selected stiffness. In the selected case, the SQC with the higher stiffness is critical with respect to the maximum stresses and the optimization can reduce the maximum stress only to 146 MPa, which is significantly higher than the optimal 118 MPa (see Fig. 10). This shows that an *a priori* selection of SQC properties based on rotor dynamics only can lead to sub-optimal fatigue life performance.

As the stiffness values of the two SQCs are varied during the optimization process, the critical speed that is optimized may shift to higher or lower frequencies, and thus, interchange with another critical speed. In these cases, it is important to use a method that can always find the same critical speed, i.e., a method that uses the MAC criterion [14]. Fig. 11 shows the

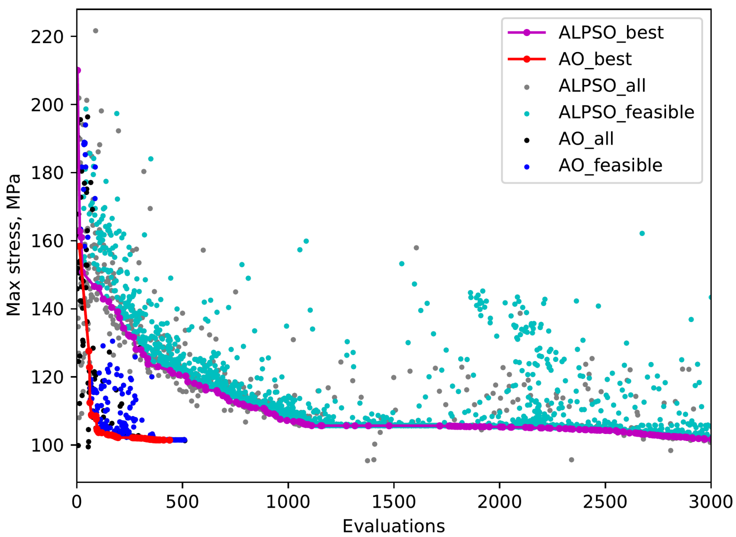

Fig. 9. Reduction of maximum stress in SQCs by AutoOpti and ALPSO optimizers with variable N_{bars}

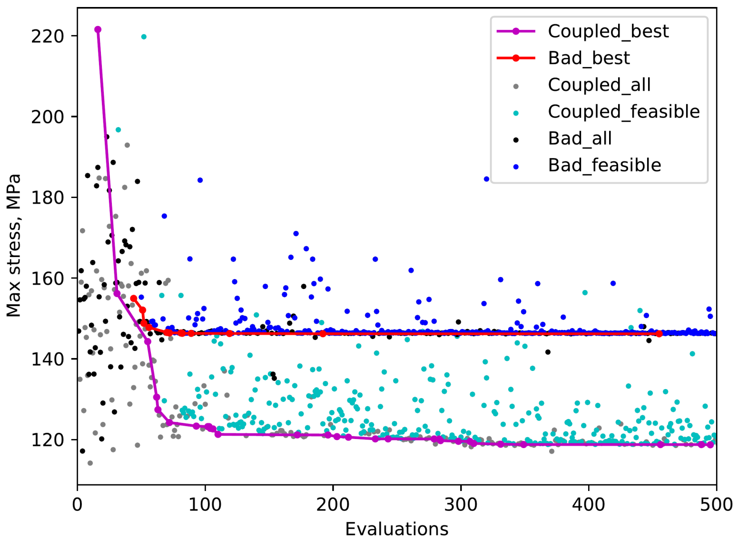

Fig. 10. Example of possible non-optimal (”bad”) SQC stiffness selection based on rotor dynamics only

Campbell diagram after the optimization of the SQCs. In this work, the critical speed to be optimized was always far enough away from the other critical speeds of the system, so no MAC criterion was needed.

6. Squirrel cage fatigue behavior

In this section, the fatigue life performance of several optimized and non-optimized SQC designs is compared. The high cycle fatigue (HCF) is analyzed using the Haigh diagram. Squirrel cages are usually subjected to axial loads, but they will be ignored in this case. The influence of the axial loads (with constant or varying magnitude) on the SQC stresses can be easily included in the current approach. Only squirrel cage 1 (SQC1) will be considered for the analysis of results, as the second SQC has essentially the same optimized design. For the calculation of the HCF, the alternating and the mean stresses should be calculated. As only critical speed analysis is performed, there is no information on the actual SQC deflection due to engine vibrations. Therefore, its maximum allowable vibration (orbiting) is considered in the following. The maximum radial displacement of the squirrel cage is limited to the maximum squeeze film gap, which in this case is 120 μm. The mean stress in this case is merely due to the weight of the engine. A static calculation is performed and the static deflection at the squirrel cage position is obtained. At SQC1, a static deflection of 8 μm is obtained. Assuming a mono-frequency com-

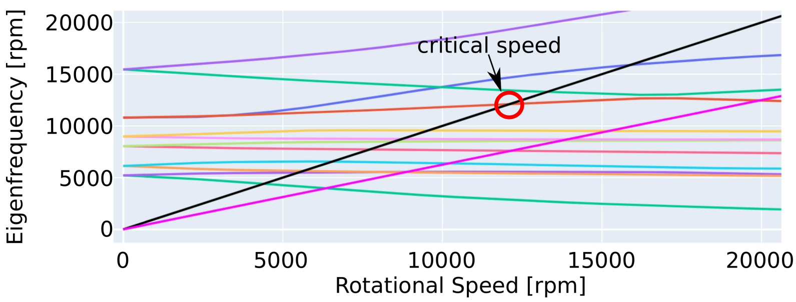

Fig. 11. Campbell diagram of the optimized rotor/bearing/casing system

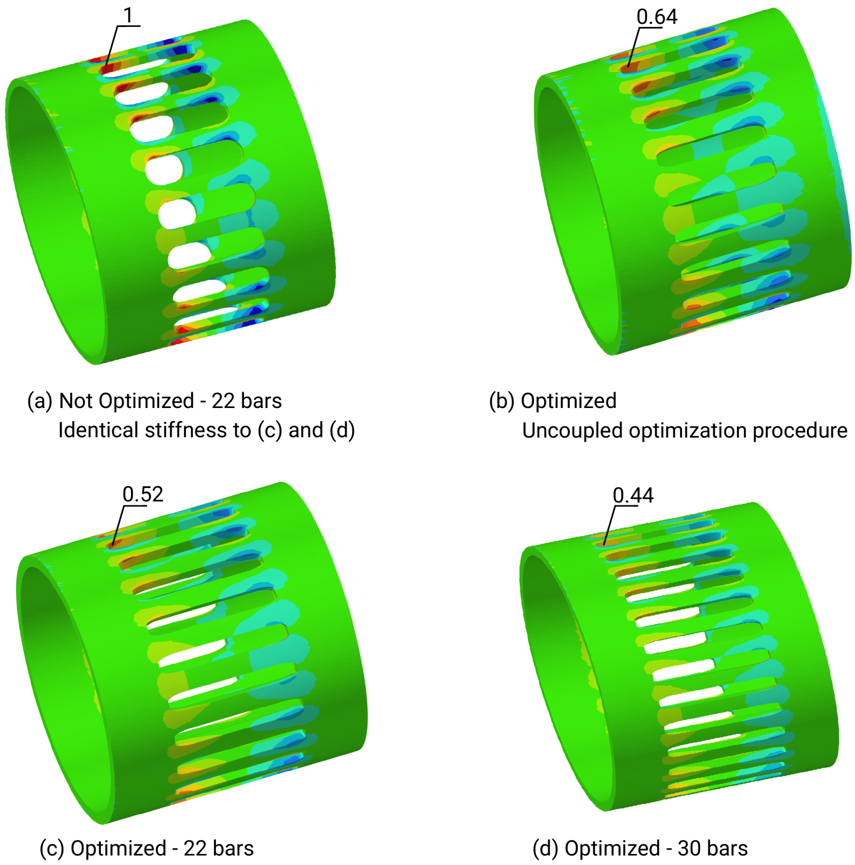

(a) Not Optimized - 22 bars
Identical stiffness to (c) and (d)

(b) Optimized
Uncoupled optimization procedure

(c) Optimized - 22 bars

(d) Optimized - 30 bars

Fig. 12. Scaled worst principle stresses on the SQC 1 (scaling according to the maximum stress from the case (a)): (a) not optimized squirrel cage with the same stiffness as in cases (c) and (d); (b) optimized squirrel cage in a decoupled optimization approach; (c) optimized squirrel cage using a fixed number of 22 bars; (d) optimized squirrel cage using the number of bars as an optimization parameter

ponent orbiting of the squirrel cage, the maximum orbiting radius is 112 μm. This assumption is critical, since otherwise it is not possible to predict vibration behavior of the SQC. To show the significance of the stresses in the optimization procedure, we take the optimized bearing from Section 5 and another bearing that shows a similar stiffness value. These two squirrel cages are shown in Fig. 12. Due to intellectual property reasons, the material properties used for the Haigh diagram are fictitious.

The results for all the squirrel cages described above are shown in Fig. 13. The fatigue stress is denoted by σ_{fs}, the tensile strength by σ_{uts} and the yield strength by σ_{ys}. It can be seen that the stresses of the non-optimized SQC that fulfills the rotor dynamics requirements (Fig. 13 – point a), can be higher than the infinite life stresses given by the Goodman line. Percentage to the Goodman line is calculated as the ratio of the two arrows (where the red arrow represents the 100 % Goodman point) shown in Fig. 13. In the literature [11] and industrial applications, there are several methods for the Goodman percentage calculation as well as there are several limits that can be considered reliable. The uncoupled optimization method may also lead to sub-optimum squirrel cage designs (Fig. 13 – point b). Finally, the coupled approach using the number of bars as a fixed parameter (Fig. 13 – point c) and as an optimization parameter (Fig. 13 – point d) provides optimized rotor dynamics and squirrel cage designs with reduced Goodman ratios up to 52 % and 44 % relative to the non-optimized design, respectively.

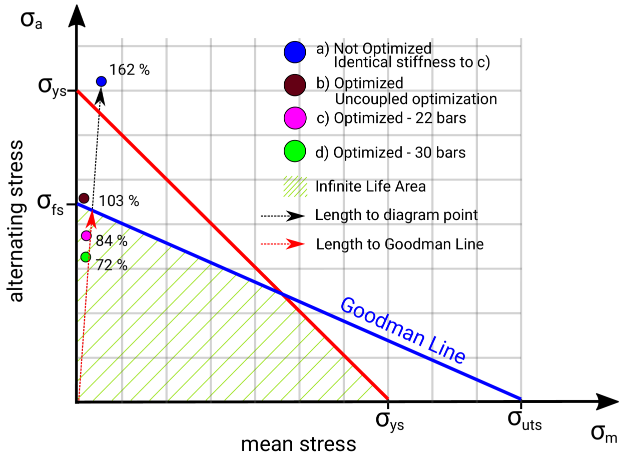

Fig. 13. Haigh diagram for the squirrel cages described in Fig. 12

7. Conclusion

In this work an end-to-end coupled rotor dynamics–squirrel cage optimization is presented and applied to the developed realistic rotor dynamics model of a two-spool aircraft engine. The developed automatized analysis process chain includes the critical speed analysis of the rotor/bearing/casing system coupled together with a 3D FEM static analysis of the two squirrel cages regarding their stiffness and stress values and allows to evaluate the effect of the SQCs geometry variation onto both disciplines.

The optimization is performed towards a robust rotor dynamics design as well as increased fatigue life of the squirrel cage. Two optimization methods were compared regarding the results as well as their efficiency. Optimization results indicate the importance of numerical optimization to improve the fatigue life of the squirrel cage, where the maximum stresses were reduced by more than 50 %. It is shown that optimized and non-optimized SQC designs, both fulfilling rotor dynamics goals, can undergo quite different fatigue during their lifespan. Moreover, the advantage of the coupled process is illustrated, allowing to find superior SQC designs by considering both disciplines simultaneously in comparison with a sequential (uncoupled) approach, when the target elastic properties of an SQC, selected only based on the rotor dynamics requirements, may lead to sub-optimal fatigue life.

In future work, additional SQC design criteria will be added, such as weight and manufacturing costs, which may require multi-objective optimization methods. At the same time, additional system parameters as well as design criteria (e.g., other modes) will be included in the rotor dynamics optimization. Another idea is to use multiple 3D SQC design optimizations to discover the dependency between the stiffness and best possible stress values for this particular geometry parameterization and to use a surrogate model to incorporate this dependency into the rotor dynamics tool. This would allow us to indirectly include stress analysis into the full system dynamics simulation at almost no additional computational costs (when compared to FEM SQC simulations).

Acknowledgement

The authors would like to thank MTU Aero Engines for allowing the publication of the current paper. All the information and methods used in this work are not necessarily in accordance with the standard work of MTU Aero Engines.

References

[1] Aulich, M., Siller, U., High-dimensional constrained multiobjective optimization of a fan stage, Proceedings of ASME 2011 Turbo Expo: Turbine Technical Conference and Exposition, Vancouver, 2011, pp. 1185–1196. https://doi.org/10.1115/GT2011-45618

[2] Braun, L., Aircraft engine rotor modelling and analyses with flexibility matrices, Master thesis, University of Stuttgart, Stuttgart, 2021.

[3] Dhondt, G., Wittig, K., CalculiX – A free software three-dimensional structural finite element program, http://www.calculix.de, November 2023.

[4] El-Shafei, A., Yakoub R. Y. K., Optimum design of squeeze film dampers supporting multiple-mode rotors, Journal of Engineering for Gas Turbines and Power 124 (4) (2002) 992–1002. https://doi.org/10.1115/1.1479338

[5] Friswell, M. I., Penny, J. E., Garvey, S. D., Lees, A. W., Dynamics of rotating machines, Cambridge University Press, 2010. https://doi.org/10.1017/CBO9780511780509

[6] Genta, G., Gugliotta, A., A conical element for finite element rotor dynamics, Journal of Sound and Vibration 120 (1) (1988) 175–182. https://doi.org/10.1016/0022-460X(88)90342-2

[7] Jansen P. W., Perez R. E., Constrained structural design optimization via a parallel augmented Lagrangian particle swarm optimization approach, Computers & Structures 89 (13–14) (2011) 1352–1366. https://doi.org/10.1016/j.compstruc.2011.03.011

[8] McKay M. D., Beckman R. J., Conover W. J., Comparison of three methods for selecting values of input variables in the analysis of output from a computer code, Technometrics 21 (2) (1979) 239–245. https://doi.org/10.1080/00401706.1979.10489755

[9] Perez R. E., Jansen P. W., Martins J. R. R. A., pyOpt: a Python-based object-oriented framework for nonlinear constrained optimization, Structural and Multidisciplinary Optimization 45 (1) (2012) 101–118. https://doi.org/10.1007/s00158-011-0666-3

[10] Schonlau M., Welch W. J., Jones D. R., Global versus local search in constrained optimizations of computer models, New Developments and Applications in Experimental Design 34 (1998) 11–25. https://doi.org/10.1214/lnms/1215456182

[11] Siemens Software, The Goodman-Haigh diagram for infinite life, 2019. https://community.sw.siemens.com/s/article/the-goodman-haigh-diagram-for-infinite-life, November 2023.

[12] Siller, U., Voß, C., Nicke, E., Automated multidisciplinary optimization of a transonic axial compressor, Proceedings of the 47th AIAA Aerospace Sciences Meeting Including The New Horizons Forum and Aerospace Exposition, Orlando, 2009, pp. 1–12. https://doi.org/10.2514/6.2009-863

[13] Srinivasan S. K. K., Periarowthar, N., Structural design and analysis of cylindrical squirrel cage to meet stiffness, strength and high cycle fatigue life for an aero engine, Proceedings of the ASME 2017 Gas Turbine India Conference, Bangalore, 2017, pp. 1–7. https://doi.org/10.1115/GTINDIA2017-4696

[14] Vacher, P., Jacquier, B., Bucharles, A., Extensions of the MAC criterion to complex modes, Proceedings of the 24th International Conference on Noise and Vibration engineering (ISMA2010), Leuven, 2010, pp. 2713–2726.

[15] Wang D., Zhang W. H., Wang Z. P., Zhu J. H., Shape optimization of 3D curved slots and its application to the squirrel-cage elastic support design, Science China Physics, Mechanics and Astronomy 53 (2010) 1895–1900. https://doi.org/10.1007/s11433-010-4093-z

[16] Zhang W., Han B., Li X., Sun J., Ding Q., Multiple-objective design optimization of squirrel cage for squeeze film damper by using cell mapping method and experimental validation, Mechanism and Machine Theory 132 (2019) 66–79. https://doi.org/10.1016/j.mechmachtheory.2018.10.010